MOLECULAR IMAGING AND BIOLOGY

Mol Imaging Biol (2019) 21:879–887
DOI: 10.1007/s11307-019-01317-6

Published Online: 1 February 2019

RESEARCH ARTICLE

Radiosynthesis and Preclinical Evaluation of an α_{2A}-Adrenoceptor Tracer Candidate, 6-[^{18}F]Fluoro-marsanidine

Anna Krzyczmonik,[1] Thomas Keller,[1] Francisco R. López-Picón,[2,3] Sarita Forsback,[1,4] Anna K. Kirjavainen,[1] Jatta S. Takkinen,[2,3] Aleksandra Wasilewska,[5] Mika Scheinin,[6] Merja Haaparanta-Solin,[2,3] Franciszek Sączewski,[5] Olof Solin[1,4,7]

[1]*Radiopharmaceutical Chemistry Laboratory, Turku PET Centre, University of Turku, Turku, Finland*
[2]*PET Preclinical Imaging Laboratory, Turku PET Centre, University of Turku, Turku, Finland*
[3]*MediCity Research Laboratory, University of Turku, Turku, Finland*
[4]*Department of Chemistry, University of Turku, Turku, Finland*
[5]*Department of Chemical Technology of Drugs, Faculty of Pharmacy, Medical University of Gdańsk, Gdańsk, Poland*
[6]*Institute of Biomedicine, University of Turku, and Unit of Clinical Pharmacology, Turku University Hospital, Turku, Finland*
[7]*Accelerator Laboratory, Turku PET Centre, Åbo Akademi University, Kiinamyllynkatu 4-8, FI-20520, Turku, Finland*

Abstract

Purpose: The α_2-adrenoceptors mediate many effects of norepinephrine and epinephrine, and participate in the regulation of neuronal, endocrine, cardiovascular, vegetative, and metabolic functions. Of the three receptor subtypes, only α_{2A} and α_{2C} are found in the brain in significant amounts. Subtype-selective positron emission tomography (PET) imaging of α_2-adrenoceptors has been limited to the α_{2C} subtype. Here, we report the synthesis of 6-[^{18}F]fluoro-marsanidine, a subtype-selective PET tracer candidate for α_{2A}-adrenoceptors, and its preclinical evaluation in rats and mice.

Procedures: 6-[^{18}F]Fluoro-marsanidine was synthesized using electrophilic F-18 fluorination with [^{18}F]Selectfluor bis(triflate). The tracer was evaluated in Sprague Dawley rats and in α_{2A}-knockout (KO) and wild-type (WT) mice for subtype selectivity. *In vivo* PET imaging and *ex vivo* brain autoradiography were performed to determine the tracer distribution in the brain. The specificity of the tracer for the target was determined by pretreatment with the subtype-non-selective α_2-agonist medetomidine. The peripheral biodistribution and extent of metabolism of 6-[^{18}F]fluoro-marsanidine were also analyzed.

Results: 6-[^{18}F]Fluoro-marsanidine was synthesized with [^{18}F]Selectfluor bis(triflate) in a radiochemical yield of 6.4 ± 1.7 %. The molar activity was 3.1 to 26.6 GBq/μmol, and the radiochemical purity was > 99 %. *In vivo* studies in mice revealed lower uptake in the brains of α_{2A}-KO mice compared to WT mice. The results for selectivity were confirmed by *ex vivo* brain autoradiography. Blocking studies revealed reduced uptake in α_{2A}-adrenoceptor-rich brain regions in pretreated animals, demonstrating the specificity of the tracer. Metabolite analyses revealed very rapid metabolism of 6-[^{18}F]fluoro-marsanidine with blood-brain barrier-permeable metabolites in both rats and mice.

Electronic supplementary material The online version of this article (https://doi.org/10.1007/s11307-019-01317-6) contains supplementary material, which is available to authorized users.

Correspondence to: Olof Solin; *e-mail:* olof.solin@abo.fi

Conclusion: 6-[^{18}F]Fluoro-marsanidine was synthesized and evaluated as a PET tracer candidate for brain α_{2A}-adrenoceptors. However, rapid metabolism, extensive presence of labeled metabolites in the brain, and high non-specific uptake in mouse and rat brain make 6-[^{18}F]fluoro-marsanidine unsuitable for α_{2A}-adrenoceptor targeting in rodents *in vivo*.

Key words: α_{2A}-adrenoceptor, PET, 6-[^{18}F]Fluoro-marsanidine, [^{18}F]Selectfluor bis(triflate), Electrophilic fluorination, Autoradiography

Introduction

The adrenergic system participates in the regulation of neuronal, endocrine, cardiovascular, vegetative, and metabolic functions. Epinephrine and norepinephrine signaling is transmitted through the cell membrane by the activation of G protein-coupled receptors [1]. These receptors are divided into three main types (*i.e.*, α_1-, α_2-, and β-adrenoceptors), each consisting three receptor subtypes [2]. The α_2-adrenoceptor subtypes α_{2A}, α_{2B}, and α_{2C} are all expressed both in the central nervous system and in peripheral tissues [3]. Pharmacological activation of central α_2-adrenoceptors results in sedation, anxiolysis, analgesia, and anesthetic-like effects [4]. Disturbances in the function of α_2-adrenoceptors have been reported in many neuropsychiatric disorders, including Alzheimer's disease [5, 6], schizophrenia [7], depression [8, 9], long-term stress responses [10, 11], and anxiety [12, 13]. Thus, α_2-adrenoceptors are potential drug targets for the treatment of neurological and psychiatric disorders.

Positron emission tomography (PET) is an imaging technique used to investigate biological processes on the molecular level. Many tracer candidates have been evaluated as α_2-adrenoceptor imaging agents. Unfortunately, many promising compounds, such as [^{11}C]MK-912 [14], [^{11}C]WY-26703 [15], [N-methyl-^{11}C]mianserin [16], and [O-methyl-^{11}C]RS-15385-197 [17], have been found not to be useful for *in vivo* imaging of α_2-adrenoceptors. More promising results have been obtained with [^{11}C]yohimbine [18], [N-methyl-^{11}C]mirtazapine [19, 20], and [^{11}C]R107474 [21]. High interest in developing subtype-selective PET ligands has resulted in the development of an α_{2A}-adrenoceptor tracer candidate, [^{11}C]MPTQ [22]. In 2014, Arponen *et al*. reported an α_{2C}-selective PET tracer, [^{11}C]ORM-13070. This tracer was evaluated in mice devoid of α_{2A}-adrenoceptors and mice lacking both α_{2A}- and α_{2C}-adrenoceptors in order to confirm its high subtype selectivity [23] and has since been introduced for human use [24].

In 2008, a new group of imidazoline derivatives, especially 1-[(imidazolidin-2-yl)imino]indazole (marsanidine) were presented and demonstrated to have high α_2-adrenoceptor/imidazoline I_1 selectivity [25]. Further studies showed that the subtype selectivity of marsanidine for α_{2A}-adrenoceptors was enhanced by introduction of a fluorine atom into its structure. 6-Fluoro-marsanidine was demonstrated to have high α_{2A}-adrenoceptor selectivity over the other two receptor subtypes. Binding affinities to recombinant human α_2-adrenoceptor subtypes were determined for fluoro-marsanidine using a subtype-non-selective antagonist radioligand, [^{3}H]RS-79948-197. The affinities of 6-fluoro-marsanidine to human α_{2A}-, α_{2B}-, and α_{2C}-adrenoceptors are 33 nM, 72 nM, and 600 nM, respectively [26]. A fluorine atom can conveniently be incorporated into the 6-position of the marsanidine structure with Selectfluor bis(triflate) [26] to obtain 6-fluoro-marsanidine, in which its F-18-labeled form constitutes a tracer candidate for α_{2A}-adrenoceptor imaging with PET.

Of the three α_2-adrenoceptor subtypes, only α_{2A} and α_{2C} are found in the brain in significant amounts. Expression of α_{2A}-adrenoceptors in mouse and rat brain is highest in regions of the brain stem and pons (locus coeruleus and pontine nuclei), hypothalamus (mammillary nuclei), septal region (lateral septum), amygdaloidal complex (medial amygdaloidal nuclei), and the olfactory system (anterior olfactory nucleus). Significantly higher expression is found in the midbrain (central gray), hippocampal region (subicular areas and entorhinal cortex), and cerebral cortex (cingulate, medial, and retrosplenial cortex) of rats compared to mice [27–29].

In the present study, 6-[^{18}F]fluoro-1-[(imidazolidin-2-yl)imino]-1H-indazole (6-[^{18}F]fluoro-marsanidine) was synthetized with moderate molar activity (A_m) and evaluated in rats and mice. The uptake of the tracer was determined in the brain and peripheral organs of both rats and mice *in vivo* using PET/computed tomography (CT) and *ex vivo* using autoradiography and organ radioactivity counting. The receptor specificity of 6-[^{18}F]fluoro-marsanidine was assessed by pretreatment with a subtype-non-selective agonist of α_2-adrenoceptors. Subtype selectivity was tested using α_{2A}-KO and WT mice. The amount of non-metabolized 6-[^{18}F]fluoro-marsanidine in plasma and brain homogenates was determined by thin-layer chromatography combined with autoradiography (radioTLC).

Materials and Methods

General

All organic HPLC solvents were HPLC grade and purchased from Sigma-Aldrich (Steinheim, Germany). Kryptofix 222 (4,7,13,16,21,24-hexaoxa-1,10-diazabicyclo[8.8.8]hexacosane) was purchased from Merck KGaA (Darmstadt, Germany). Ethanol and saline (0.9 % NaCl) for tracer formulation were purchased from Berner Oy (Helsinki, Finland) and B. Braun Medical Oy (Helsinki, Finland). The Selectfluor precursor (1-

chloromethyl-4-aza-1-azoniabicyclo[2.2.2]octane triflate) was supplied by Prof. Gouverneur's group from the University of Oxford (Oxford, United Kingdom). The 6-[^{18}F]fluoro-marsanidine precursor (1-{[1,3-di(tert-butoxycarbonyl)imidazolidin-2-yl]imino}-6-(tributylstannyl)indazole) was supplied by Prof. Saczewski's group (Medical University of Gdańsk, Gdańsk, Poland) and prepared according to the procedure reported by Wasilewska et al. [26]. Other chemicals were bought from Sigma-Aldrich (Steinheim, Germany). Oxygen-18-enriched water for fluorine-18 production was purchased from Rotem Industries Ltd. (Arava, Israel). All gases were supplied by AGA, Linde Group (Espoo, Finland).

Preparative radioHPLC was performed using a Merck Hitachi L-6200 pump with an L-7400 UV detector (at 254 nm) and 2 × 2 in. NaI(TI) scintillator detector. Analytical radioHPLC was carried out using a Merck Hitachi LaChrom 7000 system with Merck Hitachi D-7000 HPLC System Manager software (version 3.1.1).

Production of [^{18}F]Fluoride

[^{18}F]Fluoride was produced by irradiating oxygen-18-enriched water with a proton beam generated with an MGC-20 cyclotron (17 MeV, 10 μA) (Efremov Scientific Research Institute for Electrophysical Apparatus (NIIEFA), Leningrad, USSR) or with a CC-18/9 cyclotron (18 MeV, 40 μA) (D.V. Efremov Institute of Electrophysical Apparatus, St. Petersburg, Russia).

Synthesis of 6-[^{18}F]Fluoro-marsanidine

Synthesis of [^{18}F]F_2 [^{18}F]F_2 was produced as described previously [30]. [^{18}F]Fluoride was transferred to a reaction vessel containing Kryptofix 222 (22–28 mg) and K_2CO_3 (6–8 mg) in MeCN (1 ml). The reaction vessel was heated at 100 °C for 4 min under helium flow, followed by the addition of another 1 ml of MeCN. The heating under helium flow was continued for 4 min. Next, MeI in MeCN (1.0 ml, 1.5 mmol) was added to the dry Kryptofix 222/[^{18}F]KF complex, and the reaction carried out for 40 s at 100 °C. The resulting [^{18}F]MeF was purified by gas chromatography, transferred to a quartz chamber, and mixed with approximately 0.1–1 μmol of 0.5 % F_2 in neon. ^{18}F/^{19}F isotopic exchange was promoted by high-voltage electrical discharge (30–32 kV) for 10 s.

Synthesis of [^{18}F]Selectfluor bis(triflate) [^{18}F]Selectfluor bis(triflate) was synthesized according to the procedure described by Teare et al. [31]. Freshly produced [^{18}F]F_2 gas was bubbled through a solution containing 1.0 ± 0.3 mg (3.2 ± 1.0 μmol) of 1-chloromethyl-4-aza-1-azoniabicyclo[2.2.2]octane triflate and LiOTf 0.8 ± 0.1 mg (5.1 ± 0.6 μmol)) in acetone-D_6 (750 μl). The [^{18}F]Selectfluor bis(triflate) solution was used for further synthesis without purification.

Synthesis of 6-[^{18}F]Fluoro-marsanidine The stock solution of [^{18}F]Selectfluor bis(triflate) was transferred to a reaction vessel containing 6-fluoro-marsanidine precursor (8.33 ± 2.57 mg) and 2 eq of AgOTf. Approximately half of the solvent was evaporated under helium flow, and the reaction was carried out at 50 °C for 10 min. The solvent was evaporated to a volume of approximately 100 μl, and TFA (200 μl) was added. Deprotection was carried out for 10 min at 70 °C. The reaction mixture was cooled for 1 min, and the solution was neutralized with NaOH (2 M, 1 ml), diluted further with MeOH (1.5 ml), and injected onto the HPLC column.

HPLC purification was carried out using a Gemini-NX C18 column (10 × 250 mm, 5 μm, Phenomenex, Torrance, CA, USA). The product was eluted with 0.1 M ammonium acetate and MeOH solution (60:40, vol/vol) at a flow rate of 4 ml/min. The fraction containing the product was collected, diluted with water, and passed through a Waters Sep-Pak C18 PLUS cartridge (Waters Corporation, Milford, MA, USA), thereby trapping the product. The cartridge was washed with water and then 6-[^{18}F]fluoro-marsanidine was eluted with EtOH (700 μl) and diluted with saline (6.3 ml).

Radiochemical analyses were performed using a Kinetex EVO C18 column (4.6 × 100 mm, 5 μm, Phenomenex). HPLC separation was carried out with the mobile phases 0.1 M CH_3COONH_4 (A) and MeOH (B), employing the following gradient: 0–2 min 30 % B, 2–5 min 30–85 % B, 5–16 min 85 % B. The flow rate was 1 ml/min.

A_m was determined from the radioHPLC chromatogram. The UV detector response was calibrated with known amounts of 6-fluoro-marsanidine. The radioactive fraction corresponding to the product was collected and its radioactivity measured, and the area of the corresponding UV peak was determined. The amount of 6-fluoro-marsanidine was calculated by comparing the areas of the UV peaks in calibration and analytical chromatograms.

Animals and Ethical Statement Animal studies were performed on locally outbred male Sprague Dawley rats (originally from Harlan; $n = 10$, weight = 261 ± 19 g), C57BL/6J WT mice ($n = 3$, weight = 26.0 ± 5.2 g), and one α_{2A}-KO mouse (weight = 22.6 g). The α_{2A}-KO mice were originally a gift from Dr. Brian K. Kobilka (Stanford University, CA, USA) [32], and were bred locally. C57BL/6J mice were obtained from the The Jackson Laboratory (Table 1). All animals were group-housed under standard conditions (temperature 21 ± 3 °C, humidity 55 ± 15 %, lights on from 6:00 a.m. until 6:00 p.m.) at the Central Animal Laboratory, University of Turku, Turku, Finland. The study was approved by the Regional State Administrative Agency for Southern Finland (license number ESAVI/3899/04.10.07/2013).

In Vivo PET/CT Imaging and Analysis of PET Data For *in vivo* studies, rats and mice were anesthetized with a isoflurane/oxygen mixture and injected intravenously with

Table 1. Overview of animals used in the experiments. A_m, molar activity at the time of injection; A, injected activity; SD, Sprague Dawley; WT, wild type

	N	ΔTime (min)	A_m (GBq/μmol)*	A (MBq)	Injected mass (μg/kg)
SD rats	4	60	11.8 ± 6.7	20.3 ± 9.4	2.9 ± 3.3
SD rats	4	15	10.3 ± 7.7	18.0 ± 12.0	2.8 ± 3.0
SD rats blocked	2	15	19.5	31.4	1.5
			18.6	10.7	0.5
α_{2A}-KO mouse	1	60	2.5	6.6	25.1
WT mouse 1	3	60	2.5	6.5	28.3
WT mouse 2			4.2	3.1	5.8
WT mouse 3			4.2	3.2	5.6

6-[^{18}F]fluoro-marsanidine. Two rats were selected for blocking studies in order to determine the specificity of tracer uptake (Table 1). The animals were injected with a high dose of medetomidine (Cepetor, CP Pharma, Germany; 1 mg/ml; 0.5 mg/kg, ip), a subtype-non-selective agonist of α_2-adrenoceptors, 15 min before administration of the tracer. All animals were imaged by CT for 10 min for attenuation correction and anatomical reference. Four rats and all four mice were imaged immediately after tracer injection by a 60-min dynamic PET scan, and two rats used for blocking studies were imaged for 15 min. The Inveon Multimodality PET/CT scanner (Siemens Medical Solutions, Knoxville, TN, USA) has a 12.7-cm axial field of view (FOV) and 10-cm transaxial FOV, generating images from 159 transaxial slices. Frames were taken at the following intervals: 30 × 10 s, 15 × 60 s, 4 × 300 s, and 2 × 600 s for the 60-min scan and 30 × 10 s and 10 × 60 s for the 15-min scan.

For image analyses, an average rat or mouse MRI template was co-registered with PET/CT images and used as anatomical reference. Volumes of interest (VOIs) were delineated manually on the whole brain (WB), hippocampus (HIPP), hypothalamus (HYP), neocortex (CTX), and striatum (STR) using Inveon Research Workplace 4.2 (Siemens Medical Solution), and the mean radioactivity uptake values were analyzed as standardized uptake values (SUVs).

Ex Vivo Biodistribution of 6-[^{18}F]Fluoro-marsanidine and Brain Autoradiography Rats were sacrificed immediately after the *in vivo* scans by cardiac puncture under increased isoflurane anesthesia at 60 min ($n = 4$) or 15 min ($n = 2$, previously pretreated with medetomidine). *Ex vivo* rats were sacrificed 15 min ($n = 4$) after tracer injection. All mice ($n = 4$) were sacrificed after the *in vivo* scans 60 min after tracer administration (Table 1). Organs and tissues of interest were immediately dissected and weighed, and F-18 radioactivity was measured in a gamma counter (Wizard^2 3 × 3 in., PerkinElmer, Turku, Finland).

After dissection, the brains were frozen with isopentane chilled on dry ice. Coronal cryosections (20 μm) were obtained using a CM3050S cryostat (Leica Biosystems, Nussloch, Germany). Sections were collected on microscope slides, air dried, and apposed to an imaging plate (Imaging Plate BAS-TR2025; Fujifilm Corporation, Tokyo, Japan). The plates were exposed for approximately 4 h and scanned at a resolution of 25 × 25 μm using a Fuji BAS-5000 Analyzer (Fujifilm Corporation). The images were analyzed using AIDA Image Analyzer 4.5 software (Raytest Isotopenmessgeräte, Straubenhardt, Germany). Regions of interest (ROIs) were drawn over the lateral septum (LS), olfactory bulb (OB), and the striatum (STR) in mice, and over the same regions plus the locus coeruleus (LC) in rats. Region-to-striatum radioactivity ratios were calculated. The striatum was used as a reference tissue because of its low density of α_{2A}-adrenoceptors [27]. At least five sections were analyzed for each brain region of each animal, and background count densities (photostimulated luminescence per unit area, PSL/mm^2) were subtracted.

RadioTLC Analyses of 6-[^{18}F]Fluoro-marsanidine and Its Radioactive Metabolites in Plasma and Brain Cardiac blood samples were collected into lithium heparin gel tubes (Microtainer, Becton Dickinson & Co., Franklin Lakes, NJ, USA) and centrifuged (12,000×*g*, 4 min). Plasma was separated and plasma proteins were precipitated with addition of MeOH and centrifugation (12,000×*g*, 4 min). Supernatants (5–10 μl) were spotted onto the TLC Silica gel 60 RP-18 $F_{254}S$ plate (EMD Millipore 1.05559.0001, Merck Millipore, Darmstadt, Germany).

Samples of cerebral cortex were homogenized in MeOH and centrifuged (12,000×*g*, 4 min). Supernatants (30 μl) were spotted onto the TLC plate.

The plates were developed using a mixture of dichloromethane and MeOH (9:1, vol/vol). The developed plates were dried and exposed to a BAS-TR2025 imaging plate for approximately 4 h.

After exposure, the imaging plates were scanned using the Fuji BAS-5000 reader, and the fraction of non-metabolized 6-[^{18}F]fluoro-marsanidine of the total radioactivity present in each sample was analyzed with TINA software (version 2.10 g, Raytest).

Results

Radiochemistry

[^{18}F]Selectfluor bis(triflate) was produced with [^{18}F]F_2 and resulted in 6.4 ± 0.3 GBq of the crude reaction mixture, which was used further without any purification. 6-

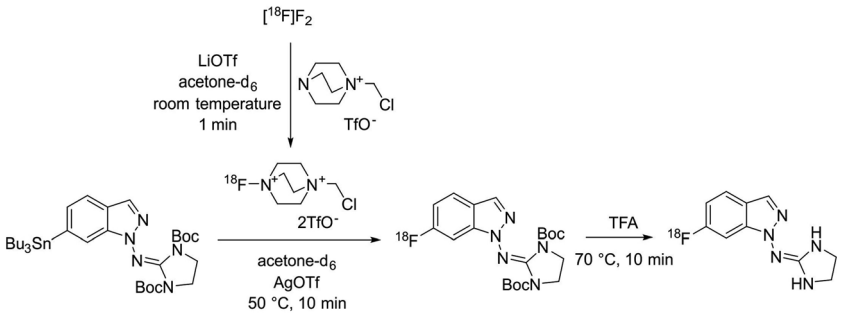

Fig. 1. Synthesis scheme for 6-[^{18}F]fluoro-marsanidine from its precursor 1-{[1,3-di(tert-butoxycarbonyl)imidazolidin-2-yl]imino}-6-(tributylstannyl)indazole and [^{18}F]Selectfluor bis(triflate). The yield for the production of 6-[^{18}F]fluoro-marsanidine from [^{18}F]Selectfluor bis(triflate) was 6.4 ± 1.7 % (radioHPLC yield).

[^{18}F]Fluoro-marsanidine was successfully produced from its precursor and [^{18}F]Selectfluor bis(triflate) (Fig. 1). The total synthesis time was 1 h 45 min. The yield was 6.4 ± 1.7 % (radioHPLC yield), and the radiochemical purity exceeded 99 %. The activity of the final product at the end of the synthesis was 256 ± 53 MBq. The A_m, at the end of the synthesis, ranged from 3.1 to 26.6 GBq/μmol and was dependent on the amount of starting radioactivity and the amount of carrier F_2 used for the high-voltage, promoted isotopic exchange.

In Vivo PET/CT

The highest F-18 activity signal in the head region of the mice was observed in the olfactory area, followed by the eyes (Fig. 2a). The level of activity in the brain of the investigated α_{2A}-KO animal was lower than that observed in WT mice (Fig. 2). Time-activity curves (TACs) in Fig. 2b illustrate the fast time course of F-18 activity uptake and washout in the brains of WT and α_{2A}-KO mice. The injected masses for the different animals were WT 1 = 28.3 μg/kg, WT 2 = 5.8 μg/kg, WT 3 = 5.6 μg/kg, and α_{2A}-KO = 25.1 μg/kg. A comparison of the shapes of the TACs within the WT group showed that the initial uptake was slower at 5 to 10 min when more 6-fluoro-marsanidine was injected, which suggests a self-blocking effect of the tracer. Noticeably, the initial uptake in the KO mouse was the lowest of all four animals (Fig. 2b). The SUVs for WB, HIPP, HYP, STR, and CTX calculated for the period 5 to 10 min were higher for the WT mice than for the α_{2A}-KO mouse (Fig. 2c). This trend was evident not only in brain regions where α_{2A}-adrenoceptors are strongly expressed, such as HIPP and HYP, but also in the WB.

Also in rats, the highest activity in the head region was seen in the olfactory area (Fig. 3a). A comparison of SUVs for the period 5 to 10 min revealed lower uptake in pretreated rats in the HIPP and HYP than in non-pretreated rats (Fig. 3b).

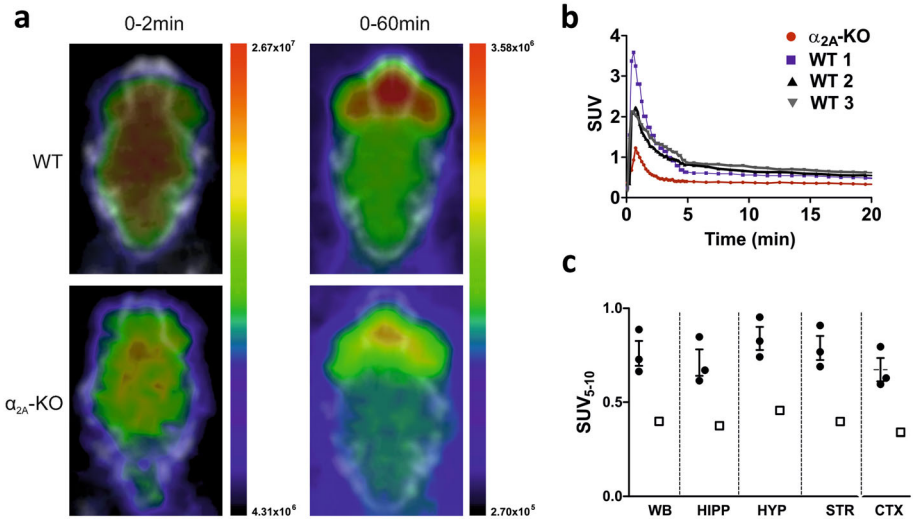

Fig. 2. **a** Representative summed maximum-intensity-projection PET/CT images show the radioactivity distribution in three wild type (WT) and one α_{2A}-KO mouse *in vivo* 0–2 min and 0–60 min after 6-[^{18}F]fluoro-marsanidine injection. The scales were adjusted separately for both time ranges. The highest uptake is seen outside the brain, in the olfactory area, and eyes. **b** Time-activity curves represent F-18 radioactivity uptake and washout in the whole brain expressed as standardized uptake values (SUVs). The injected masses for different animals were WT 1 = 28.3 μg/kg (blue), WT 2 = 5.8 μg/kg (black), WT 3 = 5.6 μg/kg (gray), and α_{2A} KO = 25.1 μg/kg (red). **c** Comparison of SUVs over 5–10 min for the whole brain (WB), hippocampus (HIPP), hypothalamus (HYP), striatum (STR), and neocortex (CTX) between the WT (●) and α_{2A}-KO (□) mice.

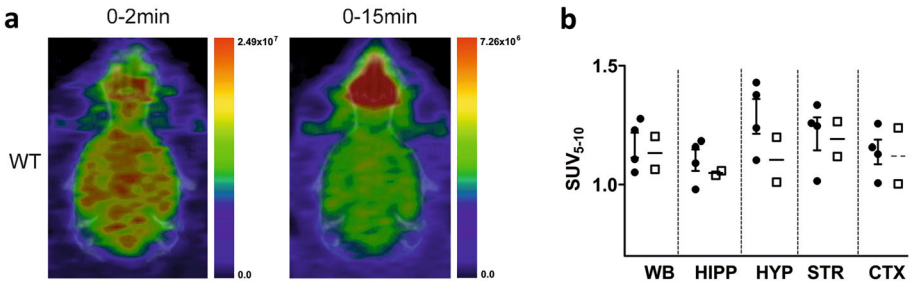

Fig. 3. **a** Summed maximum-intensity-projection PET/CT images showing the radioactivity distribution in a rat *in vivo* 0–2 min and 0–15 min after 6-[^{18}F]fluoro-marsanidine injection. The scales were adjusted separately for both time ranges. The highest activity is seen in the olfactory area. **b** Comparison of SUVs over 5–10 min for the whole brain (WB), hippocampus (HIPP), hypothalamus (HYP), striatum (STR), and neocortex (CTX) between non-pretreated (•) and pretreated (□) rats, demonstrating the effect of pretreatment with the subtype-non-selective α2-adrenoceptor agonist medetomidine.

Ex Vivo Brain Autoradiography and Biodistribution

Autoradiography of the rat brain showed that the radioactivity was lower in the STR than in the LS (Fig. 4a). Decreased LS/STR, OB/STR, and LC/STR ratios were observed in rats pretreated with medetomidine compared to non-pretreated rats at the same time point (Fig. 4c), supporting the specificity of the tracer. Analyses of *ex vivo* mouse brain autoradiographs showed that the LS and OB ratios to STR were lower for the α_{2A}-KO mouse than for the WT mice, indicating tracer selectivity for the α_{2A}-adrenoceptor subtype (Fig. 4b).

Ex vivo biodistribution studies in mice demonstrated high uptake activity in the kidneys, gallbladder, liver, stomach, and small intestine (SI). It also confirmed that the high activity signal observed in the *in vivo* scan comes from the eyes, whereas the activity in the Harderian gland (HG) was low (Fig. 5a). The peripheral biodistribution 60 min postinjection was similar in α_{2A}-KO and WT mice (data not shown).

Comparison of *ex vivo* biodistribution data obtained from rats sacrificed 15 min and 60 min after tracer injection revealed rapid washout of activity from most of the organs. In the periphery, the highest radioactivity was measured in the kidneys, liver, and SI (Fig. 5). High uptake in urine and SI indicates that 6-[^{18}F]fluoro-marsanidine and its metabolites are excreted *via* both the urinary tract and hepatobiliary tract. Low uptake in the skull demonstrates that little defluorination occurs within 60 min after tracer injection (Fig. 5).

RadioTLC Analyses

In both mice and rats, the radioTLC analysis showed a high extent of metabolism of 6-[^{18}F]fluoro-marsanidine in plasma and brain tissue. In mouse and rat plasma, five different

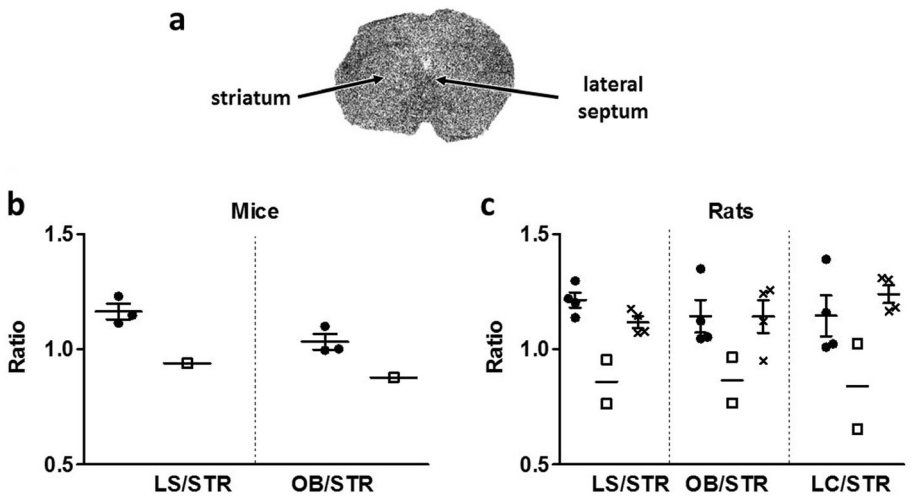

Fig. 4. **a** Representative *ex vivo* brain autoradiography image of a rat brain cryosection obtained 15 min after 6-[^{18}F]fluoro-marsanidine injection. Regions with high and low expression of α_{2A}-adrenoceptors, the lateral septum (LS), and striatum (STR), respectively, are marked with arrows. **b** Ratios of LS and olfactory bulb (OB) to STR for wild-type (•) mice and an α_{2A}-KO (□) mouse 60 min after tracer injection. **c** Ratios of LS, OB, and locus coeruleus (LC) to STR for rats were calculated from *ex vivo* autoradiographs 15 min (•) and 60 min (x) after tracer injection, and 15 min after tracer injection with medetomidine pretreatment (□).

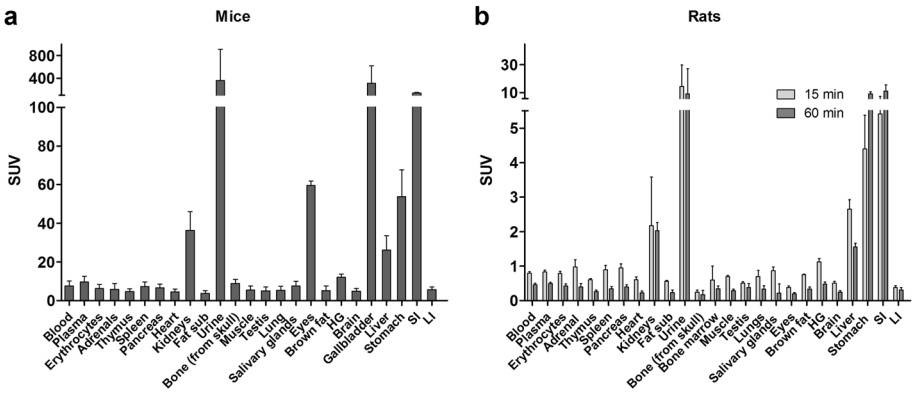

Fig. 5. **a** *Ex vivo* biodistribution of radioactivity in blood and peripheral organs of WT mice 60 min ($n = 3$) after tracer injection. **b***Ex vivo* biodistribution of radioactivity in rat blood and peripheral organs at 15 ($n = 4$) and 60 min ($n = 4$). Values are expressed as mean ± SD; HG, Harderian gland; SI, small intestine; and LI large intestine.

metabolites with retention factors (R_f) of 0.02, 0.43, 0.65, 0.83, and 0.94 were separated from the unchanged tracer ($R_f = 0.80$). In mice, after 60 min, 28.9 ± 9.3 % of the total measured radioactivity corresponded to unchanged tracer in plasma. In brain homogenates, three metabolites were separated from unchanged tracer (with R_f of 0.02, 0.65, and 0.83), and after 60 min 32.5 ± 6.7 % of the F-18 radioactivity corresponded to 6-[^{18}F]fluoro-marsanidine (Fig. 6a).

In rats, 15 min after tracer injection, only 19.2 ± 8.9 % of the radioactivity in plasma corresponded to 6-[^{18}F]fluoro-marsanidine, and this decreased to 11.1 ± 0.9 % at 60 min. In rat brain homogenates, after 15 min, 43.2 ± 12.1 % of F-18 radioactivity originated from 6-[^{18}F]fluoro-marsanidine, and this decreased to 16.8 ± 3.9 % at 60 min (Fig. 6b).

Discussion

6-[^{18}F]Fluoro-marsanidine was successfully synthesized by electrophilic F-18 fluorination with [^{18}F]Selectfluor bis(triflate). Preclinical evaluation of the tracer in both mice and rats demonstrated good blood-brain barrier penetration of the tracer and fast uptake and clearance from the brain.

The selectivity of 6-fluoro-marsanidine for human α_{2A}-adrenoceptors over the other two α_2-adrenoceptor subtypes, especially α_{2C}, was demonstrated previously [26]. The highest A_m obtained for the 6-[^{18}F]fluoro-marsanidine synthesized by the electrophilic labeling method was 26.6 GBq/μmol (at the end of the synthesis). This A_m is very high for a tracer produced by electrophilic F-18 fluorination. However, as stated in the "Results" section, comparison of the shapes of the TACs within the WT group showed that the initial uptake was slower at 5 to 10 min when more 6-fluoro-marsanidine was injected, which suggests a self-blocking effect of the tracer to some degree (Fig. 2b). The variable A_m of the 6-[^{18}F]fluoro-marsanidine led to the variation in injected masses as we injected equal radioactivity amounts in the PET studies.

RadioTLC analysis of rat and mouse plasma and brain homogenates showed rapid metabolism of 6-[^{18}F]fluoro-marsanidine. The metabolites were not identified, and their affinity to the target receptor is unknown. The fraction of unchanged tracer in plasma was approximately 30 % and 10 % of total radioactivity in mice and rats, respectively, 60 min after injection. In brain, the corresponding values at 60 min were approximately 35 % in mice and 20 % in rats.

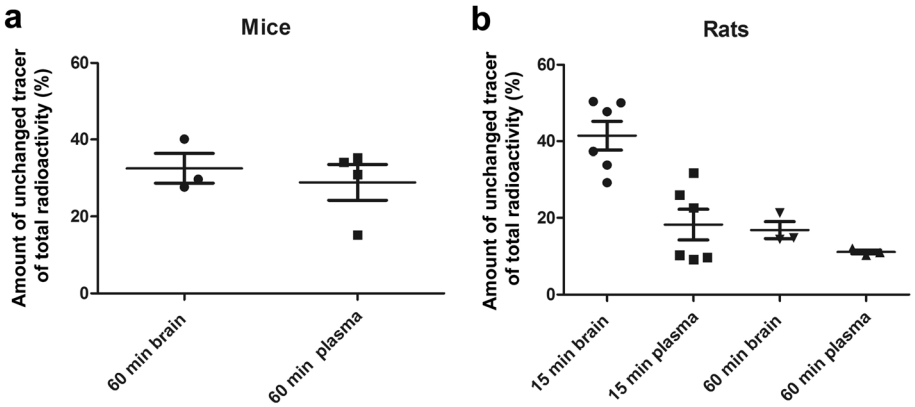

Fig. 6. Proportion of non-metabolized 6-[^{18}F]fluoro-marsanidine of the total radioactivity in plasma and brain homogenates. **a** Mice at 60 min after tracer injection. **b** Rats at 15 and 60 min after tracer injection.

The presence of radioactive metabolites in the brain causes an unspecific signal, which probably decreased the region to STR ratios in α_{2A}-adrenoceptor-rich brain regions.

In vivo studies with 6-[^{18}F]fluoro-marsanidine showed a clear difference in F-18 radioactivity uptake between α_{2A}-KO and WT mice. The *ex vivo* brain autoradiographs showed that the uptake in α_{2A}-adrenoceptor-rich brain regions, such as the LS and OB, was lower for the tested α_{2A}-KO mouse than for the WT control mice, evidently due to a lack of target for the tracer in the α_{2A}-KO brain, attesting to the selectivity of 6-[^{18}F]fluoro-marsanidine. The specificity of 6-[^{18}F]fluoro-marsanidine was demonstrated in rats following the administration of a high dose of a subtype-non-selective α_{2A}-adrenoceptor agonist. Due to the fast metabolism of the tracer and the amount of radiometabolites in the brain, and concern on animal welfare due to large medetomidine dose combined with isoflurane anesthesia, the scanning time was minimized. Therefore, animals used for blocking studies were sacrificed already 15 min after the tracer injection. Pretreated rats had reduced uptake of the tracer in HIPP and HYP, two brain regions with high levels of α_{2A}-adrenoceptors. Differences in F-18 radioactivity uptake in brain regions with different densities of α_{2A}-adrenoceptors, such as the LS and STR, were also clearly noticeable in the *ex vivo* brain autoradiographs. The high resolution of the *ex vivo* brain autoradiographs allowed for a precise analysis of small brain regions that are challenging to analyze in *in vivo* studies. The α_{2A}-adrenoceptor tracer [^{11}C]MPTQ was previously shown to accumulate in α_{2A}-rich brain regions in baboons *in vivo*. However, the α_{2A} selectivity of the tracer was not tested [22].

Ex vivo biodistribution studies in rats and mice revealed high F-18 radioactivity in the kidney, urine, and SI, indicating that 6-[^{18}F]fluoro-marsanidine and its metabolites are cleared *via* both urinary and gastrointestinal routes. Notably, F-18 uptake in bone was low (Fig. 5), indicating low defluorination of the tracer and its metabolites. In mice, high radioactivity was also found in the gallbladder and in the eyes. Analysis of the dynamic *in vivo* scans showed that initial uptake in the eyes of WT mice was higher than in the tested α_{2A}-KO mouse, suggesting that the eye uptake in mice is specific (Suppl. Fig. 1 in Electronic Supplementary Material). However, in rats, the uptake of F-18 radioactivity in the eyes was negligible, in spite of reports that α_{2A}-adrenoceptors are present in the somata of the ganglion cell layer and inner nuclear layer of the rat retina [33]. Reasons for this species difference in eye uptake may be related to dissimilar localization and/or expression of the α_{2A}-adrenoceptors in mouse and rat ocular tissue, or differences in the penetration of the tracer into the eye.

Conclusions

6-[^{18}F]Fluoro-marsanidine was successfully labeled *via* electrophilic F-18 fluorination and shown to be a specific and selective tracer candidate for brain α_{2A}-adrenoceptors. However, rapid metabolism, extensive presence of labeled metabolites in the brain, and high unspecific uptake in mouse and rat brain make 6-[^{18}F]fluoro-marsanidine unsuitable as a PET tracer for α_{2A}-adrenoceptor targeting in rodents.

Acknowledgments. Open access funding provided by University of Turku (UTU) including Turku University Central Hospital. The authors are grateful to Prof. Gouverneur and her research group (Chemistry Research Laboratory, University of Oxford) for providing the [^{18}F]Selectfluor bis(triflate) precursor.

Funding Information. This study was funded by the European Community's Seventh Framework Programme (FP7-PEOPLE-2012-ITN-RADIOMI-316882) and by a grant from the Academy of Finland (no. 266891).

Compliance with Ethical Standards. The study was approved by the Regional State Administrative Agency for Southern Finland. License number: ESAVI/3899/04.10.07/2013. All applicable institutional and national guidelines for the care and use of animals were followed.

Conflict of Interest

The authors declare no conflicts of interest.

References

1. Chabre O, Conklin BR, Brandon S et al (1994) Coupling of the alpha 2A-adrenergic receptor to multiple G-proteins. A simple approach for estimating receptor-G-protein coupling efficiency in a transient expression system. J Biol Chem 269:5730–5734
2. Bylund D, Eikenberg D, Hieble J et al (1994) International Union of Pharmacology nomenclature of adrenoceptors. Pharmacol Rev 46:121–136
3. Saunders C, Limbird LE (1999) Localization and trafficking of α2-adrenergic receptor subtypes in cells and tissues. Pharmacol Ther 84:193–205
4. Gilsbach R, Hein L (2012) Are the pharmacology and physiology of α_2-adrenoceptors determined by α_2-heteroreceptors and autoreceptors respectively? Br J Pharmacol 165:90–102
5. Kalaria RN, Andorn AC, Harik SI (1989) Alterations in adrenergic receptors of frontal cortex and cerebral microvessels in Alzheimer's disease and aging. Prog Clin Biol Res 317:367–374
6. Kalaria R, Andorn A (1991) Adrenergic-receptors in aging and Alzheimer's disease: decreased alpha-2-receptors demonstrated by [^{3}H]p-aminoclonidine binding in prefrontal cortex. Neurobiol Aging 12:131–136
7. Brosda J, Jantschak F, Pertz HH (2014) α_2-Adrenoceptors are targets for antipsychotic drugs. Psychopharmacol 231:801–812
8. Meana J, Barturen F, Garro M et al (1992) Decreased density of presynaptic alpha-2-adrenoceptors in postmortem brains of patients with Alzheimer's disease. J Neurochem 58:1896–1904
9. Cottingham C, Wang Q (2012) α_2 adrenergic receptor dysregulation in depressive disorders: implications for the neurobiology of depression and antidepressant therapy. Neurosci Biobehav Rev 36:2214–2225
10. Flügge G (1996) Alterations in the central nervous α_2-adrenoceptor system under chronic psychosocial stress. Neuroscience 75:187–196
11. Flügge G, van Kampen M, Meyer H, Fuchs E (2003) α_{2A} and α_{2C}-adrenoceptor regulation in the brain: α_{2A} changes persist after chronic stress. Eur J Neurosci 17:917–928

12. Sevy S, Papadimitriou G, Surmont D et al (1989) Noradrenergic function in generalized anxiety disorder, major depressive disorder, and healthy-subjects. Biol Psychiatry 25:141–152
13. Cameron OG, Abelson JL, Young EA (2004) Anxious and depressive disorders and their comorbidity: effect on central nervous system noradrenergic function. Biol Psychiatry 56:875–883
14. Shiue C, Pleus RC, Shiue GG, Rysavy JA, Sunderland JJ, Cornish KG, Young SD, Bylund DB (1998) Synthesis and biological evaluation of [^{11}C]MK-912 as an α_2-adrenergic receptor radioligand for PET studies. Nucl Med Biol 25:127–133
15. Pleus R, Shiue C, Shiue G, Rysavy JA, Huang H, Cornish KG, Sunderland JJ, Bylund DB (1992) Synthesis and biodistribution of the α_2-adrenergic receptor antagonist [^{11}C]WY26703. Use as a radioligand for positron emission tomography. Receptor 2:241–252
16. Marthi K, Bender D, Watanabe H, Smith DF (2002) PET evaluation of a tetracyclic, atypical antidepressant, [*N*-methyl-^{11}C]mianserin, in the living porcine brain. Nucl Med Biol 29:317–319
17. Hume SP, Hirani E, Opacka-Juffry J, Osman S, Myers R, Gunn RN, McCarron JA, Clark RD, Melichar J, Nutt DJ, Pike VW (2000) Evaluation of [O-methyl-^{11}C]RS-15385-197 as a positron emission tomography radioligand for central α_2-adrenoceptors. Eur J Nucl Med 27:475–484
18. Jakobsen S, Pedersen K, Smith DF, Jensen SB, Munk OL, Cumming P (2006) Detection of α_2-adrenergic receptors in brain of living pig with ^{11}C-Yohimbine. J Nucl Med 47:2008–2015
19. Marthi K, Jakobsen S, Bender D, Hansen SB, Smith SB, Hermansen F, Rosenberg R, Smith DF (2004) [N-methyl-^{11}C]Mirtazapine for positron emission tomography neuroimaging of antidepressant actions in humans. Psychopharmacology 174:260–265
20. Marthi K, Bender D, Gjedde A, Smith DF (2002) [^{11}C]Mirtazapine for PET neuroimaging: radiosynthesis and initial evaluation in the living porcine brain. Eur Neuropsychopharmacol 12:427–432
21. Van der Mey M, Windhorst AD, Klok RP et al (2006) Synthesis and biodistribution of [^{11}C]R107474, a new radiolabeled α_2-adrenoceptor antagonist. Bioorg Med Chem 14:4526–4534
22. Prabhakaran J, Majo VJ, Milak MS, Mali P, Savenkova L, Mann JJ, Parsey RV, Kumar JSD (2010) Synthesis and in vivo evaluation of [^{11}C]MPTQ: a potential PET tracer for α_{2A}-adrenergic receptors. Bioorg Med Chem Lett 20:3654–3657
23. Arponen E, Helin S, Marjamäki P et al (2014) A PET tracer for brain α_{2C} adrenoceptors, ^{11}C-ORM-13070: radiosynthesis and preclinical evaluation in rats and knockout mice. J Nucl Med 55:1171–1177
24. Lehto J, Virta J, Oikonen V et al (2015) Test–retest reliability of ^{11}C-ORM-13070 in PET imaging of α_{2C}-adrenoceptors in vivo in the human brain. Eur J Nucl Med Mol Imaging 42:120–127
25. Saczewski F, Kornicka A, Rybczyńska A et al (2008) 1-[(Imidazolidin-2-yl)imino]indazole. Highly α_2/I_1 selective agonist: synthesis, X-ray structure, and biological activity. J Med Chem 51:3599–3608
26. Wasilewska A, Sączewski F, Hudson AL, Ferdousi M, Scheinin M, Laurila JM, Rybczyńska A, Boblewski K, Lehmann A (2014) Fluorinated analogues of marsanidine, a highly α_2-AR/imidazoline I_1 binding site-selective hypotensive agent. Synthesis and biological activities. Eur J Med Chem 87:386–397
27. Wang R, MacMillan LB, Fremeau RT Jr et al (1996) Expression of α_2-adrenergic receptor subtype in mouse brain: evaluation of spatial and temporal information imparted by 3 kb of 5′ regulatory sequence for the α_{2A}-AR-receptor gene in transgenic animals. Neuroscience 74:199–218
28. MacDonald E, Scheinin M (1995) Distribution and pharmacology of α_2-adrenoceptors in the central nervous system. J Physiol Pharmacol 46:241–258
29. Scheinin M, Lomasney J, Hayden-Hixon D et al (1994) Distribution of α_2-adrenergic receptor subtype gene expression in rat brain. Mol Brain Res 21:133–149
30. Bergman J, Solin O (1997) Fluorine-18-labeled fluorine gas for synthesis of tracer molecules. Nucl Med Biol 24:677–683
31. Teare H, Robins E, Kirjavainen A et al (2010) Radiosynthesis and evaluation of [^{18}F]Selectfluor bis(triflate). Angew Chem Int Ed 49:6821–6824
32. Hein L, Altman JD, Kobilka BK (1999) Two functionally distinct α_2-adrenergic receptors regulate sympathetic neurotransmission. Nature 402:181–184
33. Woldemussie E, Wijono M, Pow D (2007) Localization of α_2 receptors in ocular tissues. Vis Neurosci 24:745–756